A PHENOMENOLOGICAL MODEL FOR THE MECHANICAL RESPONSE OF A SHORT FIBER REINFORCED THERMOPLASTIC

A. Andriyana, N. Billon, L. Silva
MINES-ParisTech, CEMEF - UMR CNRS 7635
1 rue Claude Daunesse, 06904 Sophia Antipolis, France
andri.andriyana@mines-paristech.fr

SUMMARY

The present work can be regarded as a first step toward an integrated modeling of mold filling during injection molding of industrial polymer composite parts and the resulting mechanical response under service loading condition. To this end, a set of experiments which captures the mechanical behavior of a short fiber reinforced thermoplastic under different strain histories is described and a three-dimensional simple phenomenological model to represent experimentally-observed response is developed. The emphasis is laid on the account of local fiber orientation in the ground matrix on the prediction of the mechanical response of the composite. The model is based on assumption that the strain energy function of the composite is given by a linear mixture of the strain energy of each constituent: an isotropic part representing the Phase 1 which is essentially related to the ground matrix and an anisotropic part describing the Phase 2 which is mainly related to the fibers and the interphase as a whole. The efficiency of the model is assessed and perspectives are drawn.

Keywords: Short fiber reinforced thermoplastic, constitutive modeling, continuum mechanics, injection molding, mechanical behavior

1. INTRODUCTION

High corrosion resistance, ease of processing, reduced weight for high fuel efficiency and low-cost tooling are among the major driving forces behind the growing use of short fiber reinforced thermoplastics in many industrial sectors, particularly in the automotive industry such as bumper beam, dashboard and sunroof frame. Therefore, it is of great interest to have knowledge of the mechanical performances of these materials. At the macroscopic level, fiber reinforced thermoplastics exhibit strong directional dependencies. Recently, a considerable effort has been devoted to the modeling of the mechanical behavior of polymer composites. Among the earlier investigations are the works of Schapery (1968), Chan (1988), Suvorova (1985) which focused on linear viscoelastic models to describe the creep behavior and Spencer (1984) who investigated the use of invariants in the description of anisotropic response. More recently, thermodynamically consistent models for elasto-plastic, viscoelastic and viscoplastic behavior were developed. For details, the reader can consult a recent review in Andriyana et al. (2009a, 2009b).

There exist at least two different approaches in the modeling of the mechanical response of composites: Micromechanics and Continuum Mechanics approaches. In the former, knowledge of the mechanics of the constituents of the microstructure of the composite, together with knowledge of their interactions are considered in order to develop a theoretical framework that would describe the mechanics of the whole composite. A second approach is based on the macroscopic description of the material as a whole and how the composite evolves under change in the mechanical environment. Such models, referred to as phenomenological models, are a powerful and effective tool to explain various physical phenomena successfully without detailed knowledge of the complexity of the internal microstructure of biological tissues in question. We will focus on the latter throughout the present paper. Moreover, we will restrict our study to the mechanical theory, and hence only isothermal processes are considered and thermal variables such as temperature and entropy are neglected.

In the present work, the mechanical behavior of an injection molded short fiber reinforced thermoplastic is addressed. A detailed experimental investigation which probes the mechanical behavior under different loading conditions is presented in Section 2. The continuum mechanical framework of the model is presented in Section 3. In Section 4, the efficiency of the model is assessed by comparison with experimental data. Finally, concluding remarks are given in Section 5.

2. EXPERIMENTAL OBSERVATION

Material and procedure

360 x 100 x 3 mm3 plates of a thermoplastic reinforced by 30 wt% of short glass fibers were injection molded with a 40°C mold temperature. Its linear viscoelastic properties in the injection flow direction was investigated by means of Dynamic Mechanical Analysis (DMA) in flexion loading mode. It was found that the α transition temperature is located around 60 to 70°C and the storage modulus varies from 3.8 to 7.8 GPa depending on temperature and frequency. At this point, it is concluded that the material exhibits a macroscopic viscoelastic behavior at small strain: the storage modulus depends on strain rate and temperature.

In an attempt to gain additional insight into the time-dependent anisotropic behavior of this composite, experiments probing the mechanical behavior, i.e. uniaxial tension tests, were conducted. The tests were performed using a computer controlled *Instron* servohydraulic uniaxial testing machine operated in strain rate control mode using a video extensometer. The specimens were obtained by tooling the plates to get geometry as illustrated in Fig. 1.

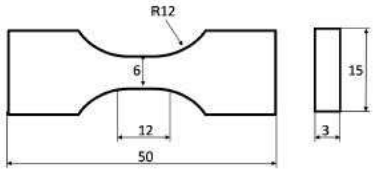

Figure 1. Specimen geometry for uniaxial tension tests.

During the tests, the specimens were subjected to various strain histories. All tests were carried out at room temperature. It is to note that all stresses in this work are presented in normalized values unless otherwise specified.

Testing results

Fig. 2 (left) presents the material behavior when subjected to a uniaxial tension at a constant strain rate of 10^{-4} s^{-1} for different specimen orientations with respect to injection flow. As expected, the material exhibits strong anisotropic and non-linear responses. For a given strain level, the highest stress is obtained for the specimen whose orientation is parallel to injection flow. The corresponding result suggests that most of the fibers in plate thickness are oriented in the flow direction. In Fig. 2 (right), a weak rate-dependence of mechanical responses is highlighted. The graph indicates that the stress increases non-linearly with increasing strain rate during the uploading. Furthermore, this dependence rises with applied strain level. This low but significant dependence on strain rate is consistent with DMA analysis.

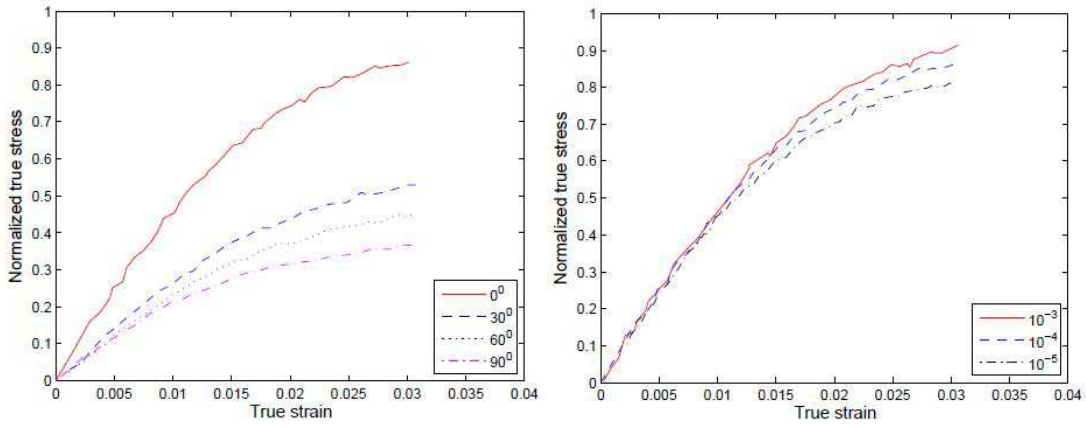

Figure 2. Mechanical response under monotonous tension test illustrating anisotropic (left) and rate dependent (right) behavior.

The time-dependence of the material can also be probed with experiments of the type illustrated in the inset of Fig. 3 (left) where at constant strain rate, the uploading and the unloading are interrupted by several relaxation segments (as also performed by Lion (1996) or Bergström and Boyce (1998) among others). The results show that during relaxation, the stress decreases in the uploading and increases in the unloading. At strain of 0.01, the time dependence is higher during the unloading than that during the uploading. An opposite trend is found at strain of 0.02 where the time-dependence during the uploading is higher than during the unloading. The evolutions of the stress during relaxation are presented in Figs. 3 (right) where stress is plotted at strain of 0.02 during the uploading and the unloading. It is shown that after 20 min of relaxation, the stress approached what appears to be an equilibrium state. Furthermore, the rate of approach towards this relaxed state is a decreasing function of the relaxation duration. It is to note that according to Lion (1996), the behavior of elastomers is characterized by a so-called equilibrium hysteresis. Thus, no unique equilibrium state, where the stress response is controlled solely by strain state, exists and consequently hysteresis may be

associated with viscoplasticity. Nevertheless, Bergström and Boyce (1998) inferred the existence of a unique equilibrium state which can be reached in the limite of in¯nite relaxation duration. In this case, the authors attributed hysteresis to viscoelasticity.

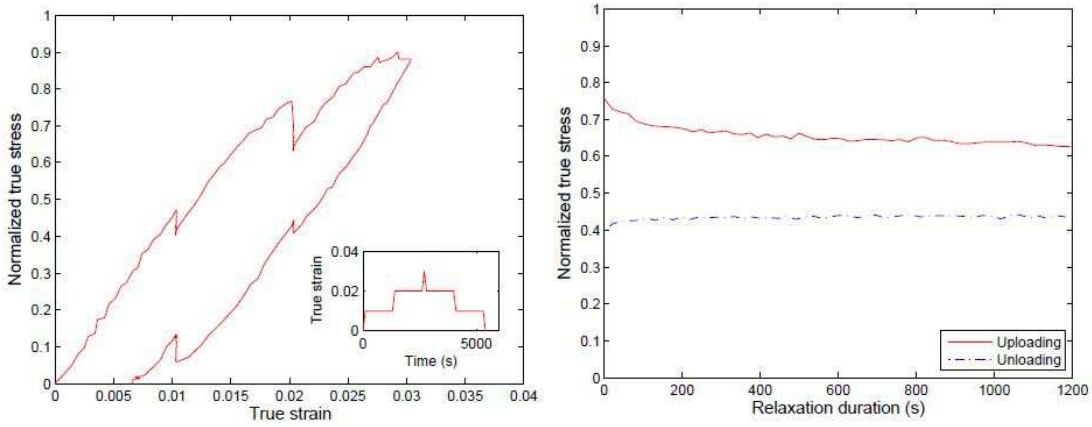

Figure 3. Left: Uploading and unloading test interrupted by several relaxations at strains of 0.01 and 0.02. Strain rate of 10^{-4} s^{-1}, relaxation duration is 1200 s. Right: Evolution of stress as a function of relaxation duration during relaxation test. Strain is 0.02.

The discussion of the experimental data has now been completed. In summary, the experimental investigation has shown that:

1. The material responses are strongly anisotropic and non-linear.
2. The time-dependent behavior is clearly marked. At relatively small strain, the dependence during the unloading is higher than during the uploading. An opposite trend is observed for higher strain.
3. The existence of a unique equilibrium state cannot be verified using our experimental time scale. Instead, the relaxed state is characterized by an equilibrium hysteresis. Further investigation by the same authors (to be published in another paper) showed that the corresponding hysteresis depends on the fiber content and orientation.

3. CONSTITUTIVE MODELING

3.1 Choice of the model

The experimental data presented in the previous section clearly demonstrated the complex behavior of this short fiber reinforced thermoplastic. The observations suggest that the mechanical response (stress) can be decomposed into two parts: an equilibrium response and a time-dependent deviation from equilibrium. The equilibrium response is decomposed into two terms as well: a non-linear elastic response and an equilibrium hysteresis which depends in a rate-independent manner on the strain history. The total stress is then simply given by the sum of these components. To address these

observations, a three-dimensional phenomenological model is developed. As highlighted in the Introduction, our approach is based on a continuum approach within the framework of multiplicative decomposition of the deformation gradient into elastic and inelastic parts. Thus, excluding micromechanical considerations.

In a continuum approach, the Representative Volume Element (RVE) has to be defined such that mechanical quantities, e.g. mass, density, stress or strain, can be represented by continuous fields. The number of phases in RVE to be accounted for in the modeling is linked to the level of complexity of the material. Mélé et al. (2002) defined three phases in a silica filled SBR: rubber matrix, silica and interphase. In fact, in the context of polymer composites, the presence of the latter phase, which is a consequence of changes in the microstructure of the ground matrix at the vicinity of the fibers (Theocaris, 1986; Alberola et al., 1999), could affect their overall mechanical response (Vendramini et al., 2000). Motivated by this observation, in the present study, the RVE is assumed to consist of two phases: *Phase 1 essentially related to the ground matrix having isotropic viscoelastic behavior and Phase 2 mainly related to the fibers and the interphase as a whole having anisotropic elasto-plastic behavior*. From a physical viewpoint, this means that inelasticity can occur at the vicinity of the fibers due to stress redistribution. From a modeling viewpoint, it allows the account of fiber orientation to the modeling of anisotropic equilibrium hysteretic response. To this end, it is postulated that the strain energy function of the composite W is given by a linear mixture of the strain energy of each constituent, i.e.

$$W = \left(1 - \upsilon_f\right) W_m + \upsilon_f W_f$$

where υ_f is the fiber volume fraction. W_m and W_f are the strain energy of the Phases 1 and 2 respectively. The form of W_m and W_f are chosen so they respect the objectivity principle (see for example in Holzapfel (2000)) and the *integrity bases* advocated by Spencer (1984).

Remark 1. *Fibers embedded in the ground matrix induce anisotropy due to their orientation. In the present work, the mechanical anisotropy is only related to fiber orientation. Hence, other phenomena which could generate anisotropy are not considered.*

Remark 2. *In fact, by writing the strain energy in the form presented above, υ_f should represent the volume fraction of the Phase 2, i.e. fibers and interphase as a whole. Nevertheless, as no experimental measurement concerning the interphase content is available, for the first approximation, it is assumed here that υ_f denotes the fiber content only.*

3.2 Kinematics

Let (C_0) be a reference configuration of the continuous body of interest. To simplify the discussion, the reference configuration is assumed to correspond to a vanishing stress and strain, stable configuration of minimum energy. Under mechanical loading, the body deforms and occupies a time sequence of physical configuration. Let (C_t) be the body configuration at time t defined by the mapping $\mathbf{x}$ ($\mathbf{X}$; t) and by its gradient $\mathbf{F}$($\mathbf{X}$; t). Furthermore, let J ($\mathbf{X}$; t) = det $\mathbf{F}$ > 0 denotes the local volume ratio. Following Flory

(1961), Lee (1969), Sidoroff (1974) and Lubliner (1985), we consider the multiplicative decompositions of the deformation gradient

$$\mathbf{F} = \mathbf{F}_{ev}\mathbf{F}_{v} = \mathbf{F}_{ep}\mathbf{F}_{p}$$

into elastic and inelastic parts where $\mathbf{F}_v$ and $\mathbf{F}_p$ are the deformation gradient which locally transform the body from the reference configuration to the intermediate configurations (C_v) and (C_p) associated respectively with the time-dependence in Phase 1 and the anisotropic equilibrium hysteresis in Phase 2. The inelastic velocity gradients $\mathbf{L}_v$ and $\mathbf{L}_p$ along with their symmetric parts $\mathbf{D}_v$ and $\mathbf{D}_p$ are defined by

$$\mathbf{L}_{v} = \dot{\mathbf{F}}_{v}\mathbf{F}_{v}^{-1} \qquad \mathbf{D}_{v} = \frac{1}{2}\left(\mathbf{L}_{v} + \mathbf{L}_{v}^{T}\right)$$

$$\mathbf{L}_{p} = \dot{\mathbf{F}}_{p}\mathbf{F}_{p}^{-1} \qquad \mathbf{D}_{p} = \frac{1}{2}\left(\mathbf{L}_{p} + \mathbf{L}_{p}^{T}\right).$$

3.3 Continuum representation of distributed fiber orientation

As emphasized previously, the only cause of mechanical anisotropy considered in the present work is the fiber orientation. Moreover, due to the nature of injection molding processes, the orientation of the short fibers embedded in the matrix at final solid state is dispersed. In order to account for distributed fiber orientations in a continuum sense, a (symmetric) generalized structural tensor (tensor of orientation) of second order is introduced and defined by (see for example Advani and Tucker (1987) for details)

$$\mathbf{A}_0 = \frac{1}{4\pi}\int_V \rho(\mathbf{a}_0)\,\mathbf{a}_0 \otimes \mathbf{a}_0 \, dV$$

where $\rho(\mathbf{a}_0)$ is an orientation density function characterizing the distribution of fibers in the reference configuration with respect to the referential orientation $\mathbf{a}_0$. The latter is an arbitrary unit vector which can be written in terms of two *Eulerian* angles $\alpha \in [0; \pi]$ and $\beta \in [0; 2\pi]$ as follow (see Fig. 4)

$$\mathbf{a}_0(\alpha,\beta) = \sin\alpha\cos\beta\ \mathbf{e}_1 + \sin\alpha\sin\beta\ \mathbf{e}_2 + \cos\alpha\ \mathbf{e}_3$$

with $(\mathbf{e}_i)_{i=1;2;3}$ denote the axis of a rectangular Cartesian coordinate system.

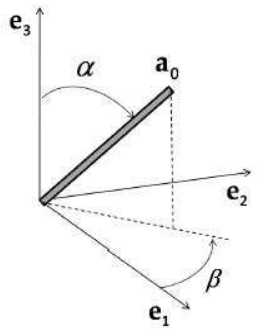

Figure 4. Characterization of an arbitrary unit direction vector $\mathbf{a}_0$ by means of *Eulerian* angles in a three-dimensional Cartesian coordinate system.

In injection molded plates, the fiber orientation state is nearly planar and no out-of-plane rotation is observed (Mlekusch, 1999; Vincent et al., 2005; Dray, 2006). Call $\mathbf{e}_3$ the axis of the plate thickness direction and $\mathbf{e}_1$ the axis of the flow direction, the tensor of orientation in this case reduces to

$$\mathbf{A}_0 = \begin{bmatrix} A_{0_{11}} & A_{0_{12}} & 0 \\ A_{0_{12}} & A_{0_{22}} & 0 \\ 0 & 0 & 0 \end{bmatrix}.$$

3.4 Stress response and evolution equations

In order to describe the stress response, we postulate the existence of a strain energy function W, defined per unit volume of the reference configuration, which depends on the strain measure $\mathbf{C}$ along with its elastic parts $\mathbf{C}_{\text{ev}}$ and $\mathbf{C}_{\text{ep}}$ as internal variables, and the fiber direction in the reference configuration $\mathbf{A}_0$. Moreover, as previously emphasized, the function W is given by a linear mixture of the strain energy of each constituent. Hence,

$$W = \left(1-\upsilon_f\right)W_m\left(\mathbf{C},\mathbf{C}_{\text{ev}}\right)+\upsilon_f W_f\left(\mathbf{C},\mathbf{C}_{\text{ep}},\mathbf{A}_0\right)$$

Considering the second law of thermodynamics, standard arguments of Coleman and Gurtin (1967) gives the Cauchy stress tensor for incompressible materials as follow

$$\boldsymbol{\sigma} = p\mathbf{I}+2\left(1-\upsilon_f\right)\left(\mathbf{F}\frac{\partial W_m}{\partial \mathbf{C}}\mathbf{F}^{\text{T}}+\mathbf{F}_{\text{ev}}\frac{\partial W_m}{\partial \mathbf{C}_{\text{ev}}}\mathbf{F}_{\text{ev}}^{\text{T}}\right)+2\upsilon_f\left(\mathbf{F}\frac{\partial W_f}{\partial \mathbf{C}}\mathbf{F}^{\text{T}}+\mathbf{F}_{\text{ev}}\frac{\partial W_f}{\partial \mathbf{C}_{\text{ev}}}\mathbf{F}_{\text{ev}}^{\text{T}}+\mathbf{F}_{\text{ep}}\frac{\partial W_f}{\partial \mathbf{C}_{\text{ep}}}\mathbf{F}_{\text{ep}}^{\text{T}}\right).$$

In the above expression, p is an indeterminate *Lagrange multiplier*, a consequence of incompressibility. It may only be determined from the equilibrium equations and the boundary conditions.

To complete the formulation, the model must be complemented by a kinetic relation which describes the evolution of the involved internal variables and the associated dissipation mechanism. Consequently, suitable evolution equations (rate equations) are required in order to describe the way irreversible process evolves. In our case, the rates of inelastic deformations have to be defined: one related to the time-dependent behavior (viscous deformation of the Phase 1) and the other associated with the equilibrium hysteresis (plastic deformation of the Phase 2).

Following Lion (1997a,b), Huber and Tsakmakis (2000) and Miehe and Keck (2000) among others, a simple fully non-linear evolution equation consistent with the second law of thermodynamics is adopted to describe evolution of the viscous deformation in the Phase 1. It is given by

$$\mathbf{D}_{\text{v}} = \frac{1}{\eta_{\text{v}}}\text{dev}\left(\mathbf{M}_{\text{ev}}\right) \qquad \mathbf{M}_{\text{ev}} = \mathbf{C}_{\text{ev}}\frac{\partial W_m}{\partial \mathbf{C}_{\text{ev}}} \qquad \eta_{\text{v}} = \eta_{\text{ov}}\exp\left(\frac{\left\|\mathbf{M}_{\text{ev}}\right\|}{s_0\left\|\mathbf{C}_{\text{ev}}\right\|^3}\right)$$

where $\mathbf{M}_{\text{ev}}$ is a stress tensor defined in the intermediate configuration (C_v) having the structure analogous to the so-called Mandel stress tensor in the plasticity theory

(Lubliner, 1986). η_v is the viscosity of the Phase 1 which is supposed to follow an exponential form.

The evolution of the rate-independent anisotropic plastic deformation in the Phase 2 is assumed to be given by the following relation

$$\mathbf{D}_{\mathrm{p}} : \widetilde{\mathbf{A}}_0 = \frac{\dot{z}}{\eta_{\mathrm{p}}} \left(2 \frac{\partial W_f}{\partial \left(\mathbf{C}_{\mathrm{ep}} : \widetilde{\mathbf{A}}_0 \right)} \mathbf{C}_{\mathrm{ep}} : \widetilde{\mathbf{A}}_0 \right) \qquad \widetilde{\mathbf{A}}_0 = \frac{\mathbf{F}_{\mathrm{p}} \mathbf{A}_0 \mathbf{F}_{\mathrm{p}}^{\mathrm{T}}}{\mathbf{C}_{\mathrm{p}} : \mathbf{A}_0}$$

where η_p is material parameter. The non-negative quantity $\dot{z} = \sqrt{\dot{\mathbf{C}} : \dot{\mathbf{C}}}$ is the time rate of the kinematic arclength (time rate of accumulated strain) so that the permanent strain depends in a rate-independent manner on the history of the total deformation (see for example Valanis (1971); Haupt and Lion (1995); Lion (1997b) for details). In contrast to classical theories of elasto-plasticity, no yield surface is introduced. Note that the structure of the above flow rule is similar to that proposed by Nguyen et al. (2007) and Nedjar (2007).

4. SIMULATIONS AND DISCUSSION

In order to determine the parameters of the model, curve fitting algorithms in combination with the trial and error method were employed. The following parameters are used throughout the simulation

Phase	Parameter	Value	Unit
Phase 1	C_1	310	MPa
	C_2	-40.62	GPa
	C_3	73	MPa
	C_4	500	MPa
	η_{ov}	210	GPa·s
	s_0	10	GPa
Phase 2	C_5	3.50	GPa
	C_6	700	MPa
	C_7	4.15	GPa
	η_p	80	MPa

Table 1. Material parameters.

The results from applying the proposed model to a uniaxial tension experiment with different strain rates is shown in Fig. 5. As illustrated, the model provides good agreements with experimental data. The rate-dependent response is well described for the strain rates of 10^{-5} s^{-1} and 10^{-4} s^{-1}. In Fig. 6, the predictions of the stress-strain response for different tensile orientations with respect to injection flow direction are presented. The applied strain rate was 10^{-4} s^{-1}. Generally, fairly good results are obtained even though the stresses are slightly underestimated. The anisotropic response is thus well described by the model.

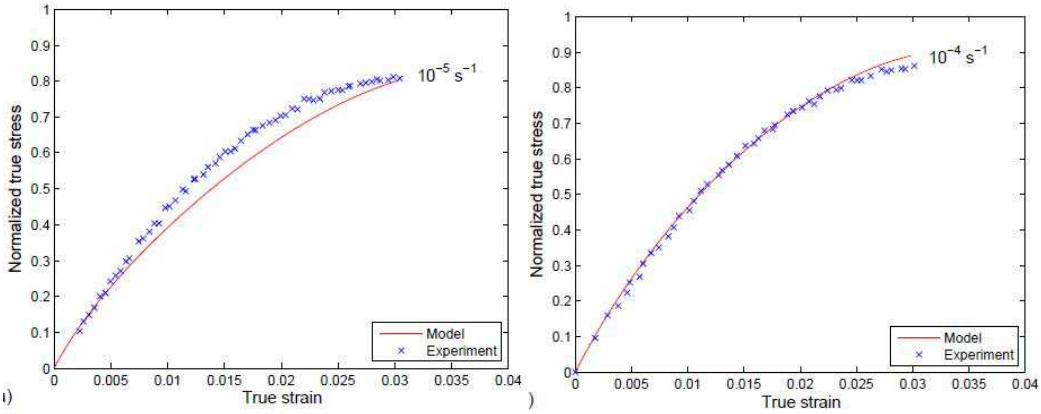

Figure 5. Numerical simulation of uniaxial tension test at orientation of 0°: strain rate of 10^{-5} s^{-1}(left) and strain rate of 10^{-4} s^{-1} (right).

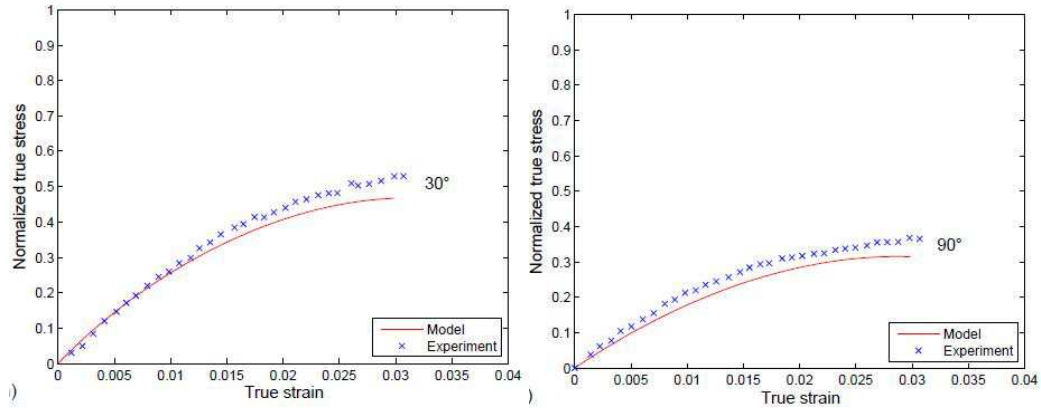

Figure 6. Numerical simulation of uniaxial tension test at strain rate of 10^{-4} s^{-1}. Orientation of 30° (left) and 90° (right).

The simulations of upload-unload interrupted with relaxations is shown in Fig. 7 (left). The model seems to give a good prediction. Furthermore, the equilibrium hysteretic response is also well represented and two opposite tendencies during relaxation are well visualized: the stress decreases in the uploading and increases in the uploading. Nevertheless, the stress response in the uploading between two segments of relaxation is slightly underestimated. Finally, the predicted rate of stress relaxation during both uploading and unloading at strain of 0.02 is shown in Fig. 7 (right). It is demonstrated that the predicted stress relaxation rate is also in good agreement with experimental data: the stress approached what appears to be an equilibrium state.

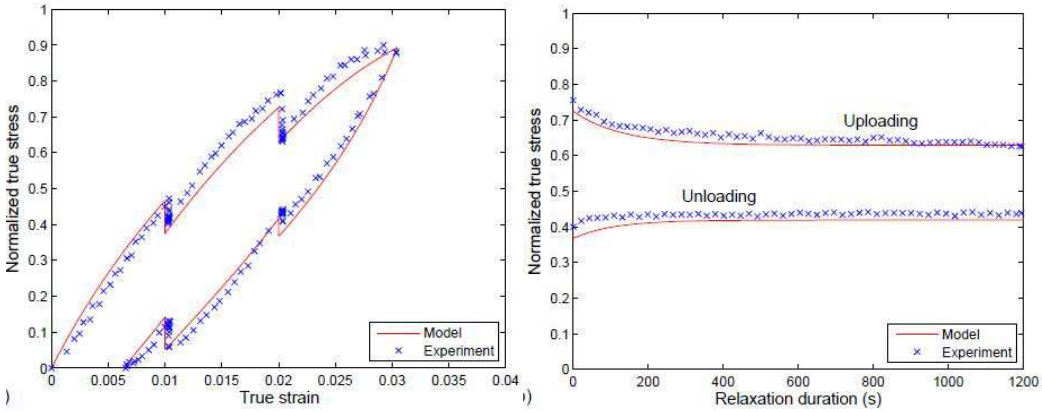

Figure 7. Numerical simulation of upload-unload test at strain rate of 10^{-4} s^{-1} interrupted by several segments of relaxation (left). Stress evolution during relaxation segment at strain of 0.02 (right).

5. CONCLUSIONS

In the present paper which is divided into two parts, the mechanical response of an injection molded short fiber reinforced thermoplastic was presented. A detailed experimental investigation which probes the mechanical behavior under different loading conditions was described and a three-dimensional phenomenological model to capture experimentally-observed response was derived. Considering experimental observation, the material is assumed to consist of two phases: Phase 1 essentially related to the ground matrix having isotropic viscoelastic behavior and Phase 2 mainly related to the fibers and the interphase as a whole having anisotropic elasto-plastic behavior. The main feature of the model is that the strain energy function of the composite is postulated as a linear mixture of the strain energy of each constituent. Comparison with experimental data showed that this simple model gives good agreements for different strain histories.

To close this paper, it is to note that specimens represent the entire thickness of the plates. Thus, the measured mechanical quantities during DMA and tension tests correspond to the average values throughout the usual skin-core layer of the material microstructure. In order to highlight the local skin-core effect, the specimens should be tooled from various locations at the plate thickness. Consequently, the question of how to tool properly the corresponding specimens arises.

ACKNOWLEDGEMENT

The authors are grateful to Dr. Gilles Robert from Rhodia for providing the material and the data of fiber orientation.

References

1. Advani, S.G. and Tucker, C.L. (1987). The use of tensors to describe and predict fiber orientation in short fiber composite. *J. Rheology*, 31:751-784.

2. Andriyana, A., Billon, N. and Silva, L. (2009a). Mechanical response of a short fiber reinforced thermoplastic. Part I: Experimental investigation. *European J. Mech. A/Solids.* (Submitted for publication).

3. Andriyana, A., Silva, L. and Billon, N. (2009b). Mechanical response of a short fiber reinforced thermoplastic. Part II: Constitutive modeling. *European J. Mech. A/Solids.* (Submitted for publication).

4. Bergström, J.S. and Boyce, M.C. (1998). Constitutive modeling of the large strain time-dependent behavior of elastomers. *J. Mech. Phys. Solids*, 46(5): 931-954.

5. Holzapfel, G.A. (2000). *Non-linear Solid Mechanics. A continuum approach for engineering*. John Wiley and Sons.

6. Huber, N. and Tsakmakis, C. (2000). Finite deformation viscoelasticity laws. *Mech. Mat.*, 32: 1-18.

7. Lion, A. (1997a). On the large deformation behaviour of reinforced rubber at different temperatures. *J. Mech. Phys. Solids*, 45: 1805-1834.

8. Lion, A. (1997b). A physically based method to represent the thermo-mechanical behavior of elastomers. *Acta Mechanica*, 123: 1-25.

9. Mélé, P., Marceaua, S., Browna, D., de Puydtb, Y., and Albérola, N. D. (2002). Reinforcement effects in fractal-structure-filled rubber. *Polymer*, 43: 5577-5586.

10. Miehe, C. and Keck, J. (2000). Superimposed finite elastic-viscoelastic-plastoelastic stress response with damage in filled rubbery polymers. Experiments, modelling and algorithmic implementation. *J. Mech. Phys. Solids*, 48: 323-365.

11. Nedjar, B. (2007). An anisotropic viscoelastic fibre-matrix model at finite strains: Continuum formulation and computational aspects. *Comput. Methods Appl. Mech. Engrg.*, 196: 1745-1756.

12. Nguyen, T. D., Jones, R. E., and Boyce, B. L. (2007). Modeling of the anisotropic finite-deformation viscoelastic behavior of soft fiber-reinforced composites. *Int. J. Solids Struct.*, 44: 8366-8389.

13. Schapery, R.A. (1968). *Stress analysis of viscoelastic composite materials*. Technomic Publishing Co., London, UK.

14. Spencer, A.J.M. (1984). Continuum theory for strongly anisotropic solids. In *Continuum Theory of the Mechanics of Fibre-reinforced Composites*, 1-32. Springer-Verlag.

15. Theocaris, P. (1986). The concept and properties of mesophase in composites. In Ishida, H. and Koenig, J. L., editors, *Composite Interface*.

16. Valanis, K. C. (1971). A theory of viscoplasticity without a yield surface. *Arch. Mech.*, 23: 517-533.